EXOTIC PARTICLES IN SMALL AND LARGE ION TRAPS*

F. Bosch, H.-J. Kluge

Gesellschaft für Schwerionenforschung (GSI)
D-64220 Darmstadt, Germany
and

Georg Bollen

CERN, CH-1211 Geneva 23, Switzerland

(Received December 8, 1995)

The storage of exotic particles like antiprotons, radioactive isotopes, or highly charged ions in ion traps or storage rings has made possible high-accuracy experiments. This publication concentrates on mass spectrometry and lifetime measurements of such species. The principle of ion storage and recent experiments will be discussed.

PACS numbers: 23.90.+w

1. Introduction

The storage of charged particles in storage rings or ion traps has a number of attractive features:

- Quite often tremendous effort has to be spent to produce rare or exotic species such as highy-charged ions, low-energy antiprotons, or radioactive isotopes. In order to make efficient use of these precious particles, it is essential to store these ions for extended periods of time.
- The procedures for injecting ions in storage rings and ion traps are now well established. They allow one to accumulate ions and thus increase signal-to-background ratios to useful levels.
- Storage devices have an inherent mass spectrometric capability. Mass resolving power of $R = M/\Delta M$ (FWHM) $> 10^9$ and accuracies in mass

* Presented at the XXIV Mazurian Lakes School of Physics, Piaski, Poland, August 23–September 2, 1995.

determination exceeding $\delta M/M = 10^{-10}$ have been obtained with Penning traps for stable isotopes [1, 2]. Mass spectrometry at storage rings has just started and has yielded resolving powers of $R > 10^5$ (see below).

- Due to high mass resolution, these stored ions can be prepared in a specific charge-over-mass state. In Penning trap [3] and storage-ring [4] experiments ground and isomeric nuclear states have for the first time been resolved by mass spectroscopy.
- Stored ions can be cooled by a large variety of different cooling techniques. Whereas in storage rings the mean velocity is high but the velocity spread very low, both become low in ion traps. As a result, brilliant beams of small phase space volume and a diameter of few millimeters are obtainable at storage rings, while ion clouds nearly at rest in a volume with 100 μm diameter are obtainable in traps. These properties are the keys for the high sensitivity and accuracy achievable by storing.
- Finally with the long storage time it is possible to measure lifetimes ranging from tens of microseconds [5, 6] to months or even years. The observation of the bound-state β-decay (see below) or the optical M1-transition in hydrogen-like ^{209}Bi ($\tau = 351$ μsec) are examples of a storage ring experiment. Lifetime measurements in ion traps have a long history and were recently reviewed by Church [7].

2. Ion traps and storage rings

The storage of charged particles both in ion traps and in storage rings originated in Europe. Whereas storage rings are still mostly a European domain, ion traps have spread out over the whole world [8, 9].

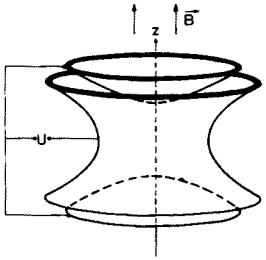

Fig. 1. Scheme of a Penning trap which consists of two hyperboloidal endcaps and a ring electrode. By a static voltage U applied between ring and caps, a quadrupole potential is created. The homogeneous magnetic field serves for radial confinement.

The principle of ion storage in Penning traps is simple [10]: The confinement of charged particles is achieved radially by a magnetic field B and

axially by a configuration of electrodes and an axially symmetric electrostatic quadrupole field like shown in Fig. 1. In general, there are three electrodes: Two end electrodes on either side of a ring electrode. All three follow the shape of the equipotential surfaces of their quadrupole potential.

Mass determination in a Penning trap is based on the measurement of the cyclotron frequency

$$\omega_c = (q/M) \cdot B \,. \tag{1}$$

Due to the electric force the motion of the ion with charge q is not a pure cyclotron motion with this frequency but a superposition of three harmonic eigen motions: An axial oscillation with frequency ω_z, a modified cyclotron motion with frequency ω_+, and a slow drift around the trap axis, called magnetron motion, with frequency ω_-. In high-accuracy mass measurements, the important relationships between the eigenfrequencies are

$$\omega_c = \omega_+ + \omega_- \text{ and } \omega_c^2 = \omega_+^2 + \omega_-^2 + \omega - z^2 \,. \tag{2}$$

For more details the reader is referred to Ref. [10].

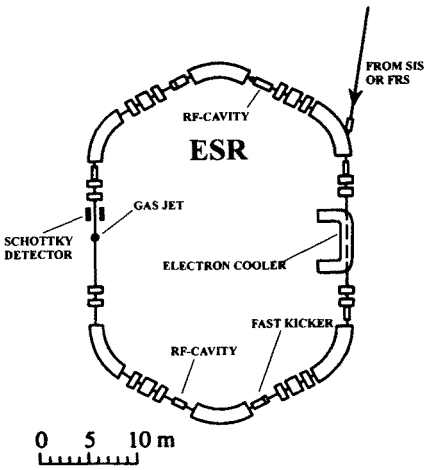

Fig. 2. Sketch of the experimental storage ring ESR at GSI. The main components for injecting and cooling of the ions are indicated as well as the gas jet target for atomic and nuclear reactions and the Schottky detector for observing the circulating ion beam. The ESR can store ions ranging from Ne^{10+} ($E \leq 834$ MeV/u) up to U^{92+} ($E \leq 556$ MeV/u).

Storage rings are devices quite similar to ion traps but scaled up in size by about three orders of magnitude. Today nine ion cooler rings are in operation [9]. The main features of storage rings will be discussed briefly using the Experimental Storage Ring (ESR) at GSI as an example. Figure

2 shows this storage ring and its main components. Stable highly-charged ions are injected into the storage ring with energies of up to 556 MeV/u for U^{92+} from the heavy ion synchrotron SIS or radioactive ions from the fragment separator FRS. By sophisticated stacking the ions are efficiently accumulated in the storage ring. By cooling (most commonly by electron cooling, see below) the phase space volume of the stored ion beam can be compressed. As a result new phase space becomes available for new ion pulses to be accumulated until the space charge limit is reached. The ions circulating in the ring with a revolution frequency of the order of 2 MHz can be observed by detecting the image charges induced in the electrodes of the so-called Schottky detector.

3. Cooling of ions in traps and storage rings

Table I gives an overview of the different techniques used to cool ions in storage rings and ion traps. Although the physics of cooling in rings and traps is identical, the technical realization is quite different for each case.

TABLE I

Cooling techniques for ions stored in storage rings and ion traps. The number of crosses indicates the extent of application of the cooling technique. Underlining indicates general applicability.

Technique	Storage Rings	Ion Traps	Example	Reference
electron cooling	xxx	x	all storage rings, $\bar{p}$	[23, 8]
positron cooling			planned for HITRAP	[14, 11]
stochastic cooling	xx		LEAR	[15, 16]
laser cooling	x	xx	Li^+, Be^+, Mg^+	[17, 24, 18]
sympathetic cooling		x	Be^+, planned for RETRAP	[19]
resistive cooling		xxx	g-2, mass spectrometry	[10, 20]
buffer gas + ω_c-excitation		x	radioactive isotopes	[21]
selection of cool ions		x	SMILE	[22]

Electron cooling [11] is the most common cooling technique and is used in all cooler rings. Here, the longitudinal velocity spread is compressed by acceleration of the electrons. The momentum spread of the stored ions is typically reduced from 10^{-3} after injection to about 10^{-6}. The ion temperature in the transverse direction is given by the temperature of the electron cathode which is $T \approx 1200$ K or 0.1 eV.

Recently, a breakthrough in electron cooling has been achieved by Danared *et al.* [12] at the CRYRING in Stockholm. Using the fact that the

ratio of the transverse energy spread and the longitudinal magnetic field is an adiabatic invariant, this group was able to reduce the transverse temperature by a factor of 10 to 10 meV by adiabatically decreasing the magnetic field from 0.3 Tesla at the electron source to 0.03 Tesla in the interaction region.

Electron cooling in ion traps has so far only been applied to antiprotons [13]. The electrons (as well as the positrons which might provide an effective cooling mechanism for highly charged ions [14]) cool themselves within a fraction of a second by synchrotron radiation in the high magnetic field of the Penning trap.

Stochastic cooling [15] has been developed for accumulation and cooling of antiprotons. It is especially efficient when the ions have a large momentum spread. It has also been tried in ion traps but convincing results have not yet been reported [16].

Laser cooling of stored ions has led to extremely low temperatures of mK and below in ion traps and storage rings [17, 18]. This technique, however, is not generally applicable since it works only in the case of very few species of singly charged ions with strong resonance transitions in a spectral region accessible by present-day laser technology. Therefore, laser cooling in storage rings has been reported only for Li^+, Be^+, and Mg^+-ions. More generally applicable is sympathetic cooling [19]. Here, simultaneously stored ions of another species are coupled by Coulomb interaction to a low-temperature bath of laser cooled ions. This cooling technique has not yet been applied to ion cooling in storage rings as it is the case for resistive cooling, where generally the energy of the axial motion is dissipated in a cooled resistor connected to the end caps [10, 20].

A new and very generally applicable technique in Penning traps for singly charged ions is buffer gas cooling in combination with a quadrupolar rf-field at the true cyclotron frequency ω_c [21]. The cyclotron motion and the z-oscillation are damped by collisions with the buffer gas, whereas the increase of the magnetron motion (which is unstable) is counteracted by rf-excitation that couples the modified cyclotron and magnetron motion. This cooling and centering technique, which is also mass-selective, has been used in the ISOLTRAP mass spectrometer at ISOLDE/CERN for mass determination of radioactive isotopes.

A brute-force technique that is not really cooling is to select cool ions by lowering the trapping potential so that the ions with high kinetic energy just leave the trap [22]. The ions remaining in the shallow potential well will have small axial amplitudes once the trapping voltage has returned to normal values. This technique is applied in the SMILE experiment for mass measurements of highly-charged ions (see below).

4. Mass spectrometry in ion traps and storage rings

Mass spectrometry is now about eighty years old. Over these years it has been developed to a precision technique allowing for accuracies far below the ppm-level which is generally accepted in physics as high accuracy. A breakthrough has been achieved during the last years: The Penning trap mass spectrometer has emerged as the most powerful instrument for mass determinations with ultra-high accuracy and the use of a storage ring has been found to be the most time efficient technique to determine masses of a large number of radioactive isotopes at an accuracy of $\delta M/M \approx 10^{-6}$.

Today, the accuracy of Penning trap mass measurements of stable isotopes reaches or even surpasses 1 part in 10^{10} [2, 25, 26]. This is achieved by using a single, singly-charged ion cooled to a temperature of liquid helium.

Such a high accuracy is required for metrology like the determination of fundamental constants or the re-definition of the kilogram on the basis of a perfect single crystal of silicon. Another example is the ^{3}H-^{3}He mass comparison which offers a constraint for neutrino mass measurements by spectrometers designed for a determination of the energy spectrum of β-particles emitted in the decay of tritium.

A sensitive test of the CPT-invariance in baryonic systems is presently performed at LEAR/CERN by a Harvard–Mainz collaboration: If this theorem holds, the masses of a particle and its antiparticle should be identical. Recently, Gabrielse, Quint *et al.* have published a mass ratio of an accuracy of 1 ppb with a single proton, respectively antiproton stored in a Penning trap at liquid helium temperature [27]. This represents by far the most accurate check of CPT-invariance in the case of baryons.

The masses of highly charged ions are determined in the Penning trap mass spectrometer SMILE installed at the electron beam ion source at Stockholm [28]. An accuracy better than 10^{-9} is reached which will provide tests of multi-configuration Dirac-Fock calculations for the atomic binding energy in few-electron systems with an accuracy of $\delta M/M \approx 100$ eV for medium-A isotopes.

4.1. Mass spectrometry of short-lived isotopes

The most fundamental property of a nucleus is its mass, *i.e.* the sum of the rest masses of the protons and neutrons minus the binding energy. All forces acting between the nucleons are showing up in the mass. Since there is presently no exact theory for strong interaction in nuclei, a large variety of nuclear models has been developed in the course of the last decades. A primary test of those models is made by comparing measured masses with calculated ones. Presently, the overall agreement between theoretical and experimental masses is in the best cases of the order of 10^{-6}. In order

to improve the models and especially their predictive power for isotopes never accessible by experiment but important for, *e.g.* nuclear synthesis, the systematic knowledge of the masses of as many as possible isotopes is required at an accuracy of 10^{-6} and better.

In the past the atomic masses of short-lived isotopes have been determined mainly by measurements of Q-values in nuclear decays and (more rarely) by nuclear reactions. First direct mass measurements by use of a Mattauch-Herzog-type mass spectrometer were performed by the Orsay group at the proton synchrotron and the ISOLDE facility at CERN [29].

During the last few years, a new generation of techniques for measuring directly masses of short-lived isotopes has evolved. One common feature of these modern techniques is a transition from the measurement of kinetic energies like in the case of Q-value determination or of voltage ratios as done in conventional mass spectrometry to a determination of time and frequency. The latter can be measured with unsurpassed accuracy.

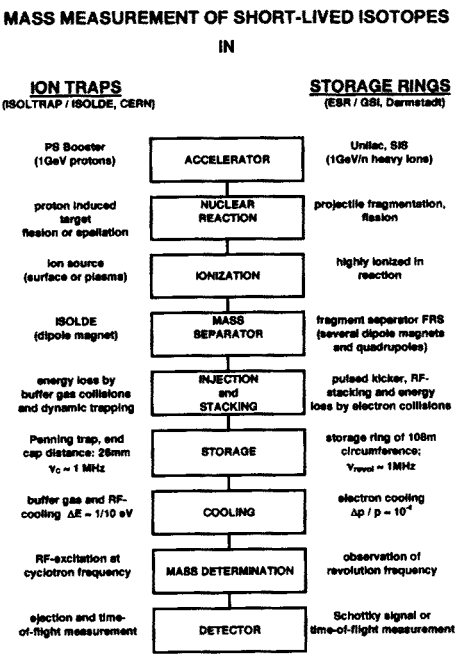

Fig. 3. Principle of mass determinations of short-lived isotopes in a Penning trap and storage ring.

In the eighties, the time-of-flight mass spectrometers TOFI [30] and SPEG [31] have been developed and installed at proton (Los Alamos) and heavy-ion (GANIL) accelerators, respectively. These novel instruments allowed the mass determination of a large number of mainly light short-lived

isotopes with a moderate resolving power of typically some thousands having a flight pass of up to nearly 100 m.

A breakthrough in high-accuracy mass spectrometry of short-lived isotopes was achieved when storage of ions for extended periods of time *and* frequency measurement were employed by ion confinement in Penning traps and storage rings. Figure 3 shows how similar the principles are for mass determinations in ion traps and storage rings.

4.1.1. The ISOLTRAP mass spectrometer at ISOLDE/CERN

The tandem Penning trap mass spectrometer ISOLTRAP [32, 33] is installed at the on-line isotope separator ISOLDE/CERN. It consists of two Penning traps. The first one serves for five functions: *(i)* accumulation of the ISOLDE beam stopped on a foil which is heated for surface ionization of the implanted sample; *(ii)* cooling of the stored ions to room temperature; *(iii)* removal of contaminating ionic species like other isotopes or isobars; *(iv)* centering the ion cloud, and *(v)* bunched ejection of the ions for transfer into the second trap.

This second Penning trap is a precision trap mounted in the very stable and homogeneous magnetic field of a superconducting coil. The ion bunch transferred from the first trap at an energy of 1 keV is captured in-flight in the precision trap. In this trap, isomeric contaminations are eliminated by accelerating those ions (like in a cyclotron) at their modified cyclotron frequency ω_+ until they collide with the ring electrode and are lost. Then, the isotope under investigation is magnetron excited to an orbit of a diameter of less than one millimeter and irradiated with radio frequency (RF) close to the expected pure cyclotron frequency ω_c. In resonance with ω_c, a conversion from magnetron motion into cyclotron motion is performed while the orbital radius remains unchanged. This RF-excitation results in an increased orbital energy which is finally detected by a reduction in the time of flight the ions need to reach a channel plate detector after pulsed ejection out of the precision trap.

The RF-interaction time of typically $T = 1$ s determines the resolving power to about $R = 10^6$ for A = 100 isotopes. Splitting the resonance curve to 10 % leads to an accuracy in mass determination of about $\delta M/M = 10^{-7}$ which corresponds to 10 keV for heavy isotopes. The maximum resolving power reached so far is $R = 10^7$ limited by the vacuum of about 10^{-9} mbar in the precision trap. Due to the limited beamtime available, ISOLTRAP is operated usually with $T = 1$ s. This enables the measurement of $A = 100$ isotopes with half lives $T_{1/2} \geq 1$ s to an accuracy of $\delta M/M = 10^{-7}$. Of course, a lower halflife limit can be obtained for lighter isotopes or by accepting a reduced resolving power. For example, for $A = 100$, $R = 10^5$, and $\delta M/M \approx 10^{-6}$, the halflife limit would be as short as $T_{1/2} \approx 10$ ms.

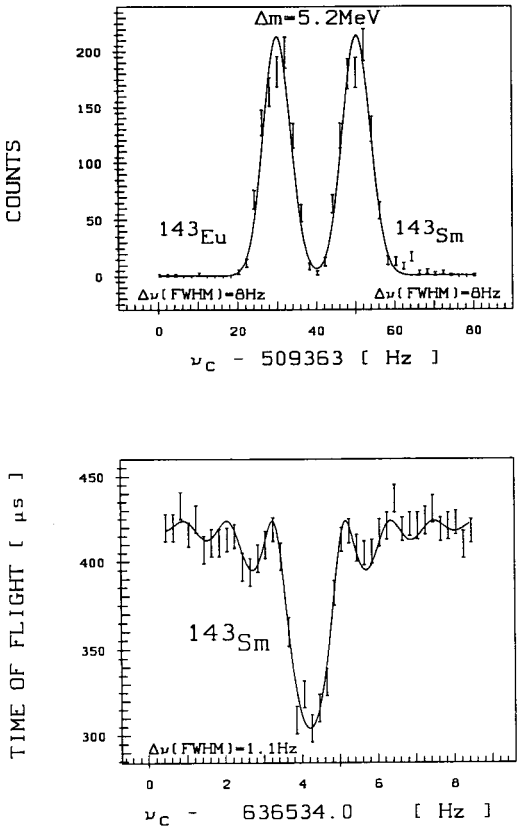

Fig. 4. Mass spectrometry of ^{143}Sm. In the first Penning trap of ISOLTRAP the contamination by ^{143}Eu (trap) is eliminated by cooling, centering, and transferring only ^{143}Sm to the second trap where the cyclotron of ^{143}Sm resonance is determined (bottom).

Until now the masses of nearly 100 isotopes have been measured by use of ISOLTRAP. As an example, Fig. 4 shows in the upper part the isobaric resolution of ^{143}Eu and ^{143}Sm in the lower trap. After cooling of only ^{143}Sm and transferring only ^{143}Sm to the precision trap, its cyclotron frequency is measured with an accuracy of 10^{-7}.

4.1.2. Schottky mass spectrometry in the experimental storage ring ESR at GSI

Very recently, it has been shown that storage rings can be used as high-resolution mass spectrometers for short-lived isotopes [34]. In fact, the ESR, having a diameter of 108 m, represents in the case of Schottky mass

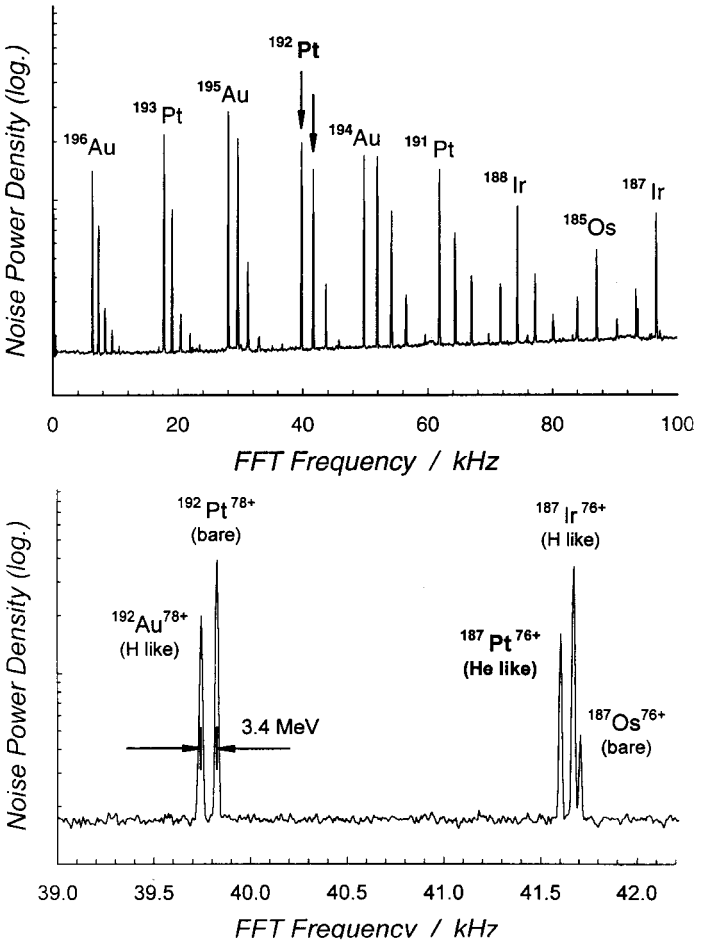

Fig. 5. Schottky mass measurement in the ESR. Highly charged isotopes are produced and mass separated in the fragment separator FRS by fragmentation of ^{197}Au. A broad-band spectrum of the Fourier transformed Schottky signal is shown at the top. The two peaks marked by arrows and by "^{192}Pt" are enlarged in the lower part. They split into five signals of two groups with almost the same q/A-ratio.

spectrometry a kind of time-of-flight spectrometer with a flight path of 10^7 km. At GSI, Au and Bi fragments produced in the fragment separator FRS were injected at relativistic energies into the experimental storage ring ESR (Fig. 2). After electron cooling to a momentum spread of $\Delta p/p = 10^{-6}$ the image current of the circulating ions are recorded and Fourier transformed into the frequency domain [35]. Even the signal of a single stored ion shows up in the rich, so-called Schottky spectrum which is made out of different

ions in various charge states (fully stripped, hydrogen-like, and helium-like (Fig. 5)). Since the velocities of the circulating ions are identical within 10^{-6}, the revolution frequencies of the different ion species are a measure of their masses. Calibrating the frequency scale by use of well known mass values, the masses of over 100 isotopes could be determined for the first time including those of some members of rather long α-chains not yet connected to the backbone of stable isotopes. Still, the data evaluation is under way. An accuracy in the range of 100 – 200 keV is obtained in a first analysis of the immense amount of data obtained representing about 10 % of the until now known masses.

Presently, the preparation of a cooled ion beam in the ESR requires around 30 s, which represents roughly the halflife limit for the nuclide under investigation. Isotopes with considerably shorter halflives will be measurable when stochastic cooling is employed as planned for 1996.

Isotopes with halflives much shorter, down to the order of milliseconds and below, will become accessible to mass spectrometry in the ESR when the ring can be operated in an isochronous mode [36]. Then the revolution frequency will be independent of the velocity of the stored ions of a single mass-over-charge ratio and no cooling will be required. Hence, the mass determination can immediately start after isotope production and separation by the FRS and when a single ion or very few ions are injected into the ESR. It is hoped that about 100 revolutions of the injected ion can be observed by detecting secondary electrons produced when the ion passes through a thin foil installed in the ring. In this mode, the ESR would represent a true time-of-flight mass spectrometer with a flight pass of about 30 km. Such an operation mode would allow a resolving power exceeding 10^5.

5. Beta lifetime measurements at storage rings

The knowledge of ground-state properties like mass and lifetime of unstable nuclei is mandatory to reveal the "paths" of nucleosynthesis in hot stellar plasmas. In the "s"-process, for example, the temperature is typically $4 \cdot 10^8$ K=30 keV and, therefore, the mean atomic charge state is high. On the other hand, the β decay probability of an atom is significantly affected by the degree of its ionization. Striking examples are orbital electron capture (EC) which trivially depends on the summed density of all bound electrons at the site of the nucleus, or the recently for the first time observed bound-state beta decay [37]. Hence, weak interaction lifetimes in a stellar plasma are *not* a priori equal to those measured in a low-temperature regime as, for instance, on the earth.

Except very few cases, β lifetimes have been determined up to now for *neutral* atoms only. Ion traps and storage rings provide for the very first

time the opportunity to investigate β lifetimes of ions in a well-defined (high) charge state. Because a considerable part of the pioneering experiments in this field have been accomplished at the ESR, we will focus in the following onto β lifetime experiments conducted there.

5.1. Beta$^+$ lifetimes of bare ions

The total lifetime of stored ions can be easily determined, just by measuring their numbers as a function of time. If, in addition, the ions are cooled, Schottky spectroscopy is obviously the ideal tool for this purpose, provided that there is a linear correspondence between the area of a specific Schottky peak and the number of related ions. This is, however, only guaranteed for a particle number below about 10^5, at least in the ESR. At higher beam intensities, additional coherent effects like plasma waves built up, disturbing thereby the linear correspondence between Schottky signal strength and ion number.

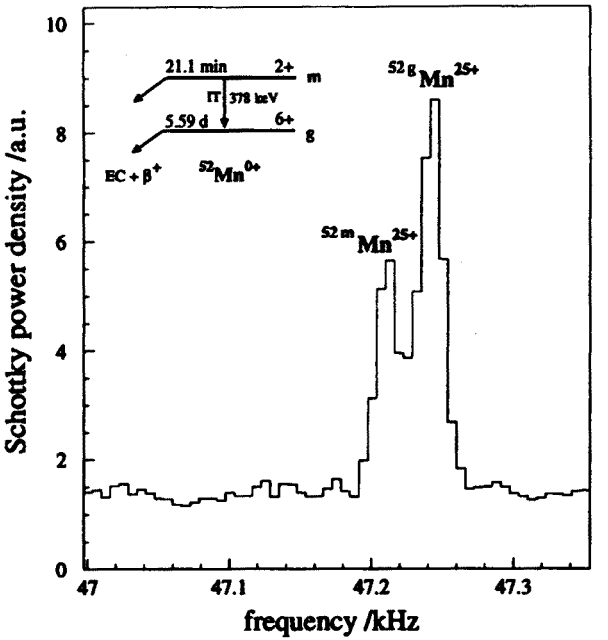

Fig. 6. Schottky spectrum of bare $^{52}Mn^{25+}$ stored and cooled in the ESR, recorded at the 21th harmonic of the revolution frequency and averaged over 40 seconds. The frequency scale denotes the difference to an admixed external frequency of 33.15 MHz. The mass-resolved lines of the ground and isomeric state ($E^* = 378$ keV) of bare $^{52}Mn^{25+}$ show a width of 21 Hz (FWHM), corresponding to a relative momentum spread of $\Delta p/p = 1.2 \cdot 10^{-6}$. The partial level scheme shown corresponds to neutral ^{52}Mn (from Ref. [4]).

The excellent resolving power of Schottky spectroscopy of *cooled* ions allows for special cases even to resolve the masses of a nuclear ground- and isomeric-state and to determine the corresponding lifetimes separately. For the case of bare $^{52}Mn^{25+}$, shown in Fig. 6 [4], the halflife of the first isomeric state which is separated from the ground state by only 378 keV, could be evaluated with an accuracy of better than 10 % from the time dependence of its Schottky peak area ($T_{1/2}$ = 23 min.). This is one example of several pure β^+ lifetimes which we addressed in a first exploratory experiment. The unique feasibility of a storage ring (or an ion trap) to store instable ions in a well-defined charge state allows, for instance, to get rid of the electron capture decay channel, just by storing *bare* ions, and to determine, therefore, the pure β^+ decay probability separately. If, in addition, the total decay probability of the neutral atom is known, one gets directly the β^+/EC-braching ratio (by applying a small correction for the Fermi function of a bare ion). Moreover, by this method very weak β^+ decay channels might be detected, too.

For highly charged ions (charge state q = Z, $Z - 1$, $Z - 2$, where Z is the proton number) and for $Z \geq 30$, the Schottky lifetime spectroscopy provides a second advantage in the ESR: For these cases the $\beta^{\pm}$-daughter still remains in the acceptance of the ring (Δ(q/A) $\approx$ 3 %) and generates its own Schottky signal. Therefore, the number of both the mother and daughter ions may be observed *simultaneously*, which reduces drastically the systematical error of lifetime determination.

The intensity of stored ions does not only change because of nuclear (beta) decay, but also because of atomic interaction with the cooler electrons and with the atoms of the residual gas. In order to get the *true nuclear* lifetime, one has to correct the measured total lifetime for these "beam-losses", by observing, for instance, the time dependence of the number of simultaneously stored *stable* ions. This procedure is shown in Fig. 7 [4], where the observed total decay probability λ_{obs} of bare $^{52}Fe^{26+}$ is corrected for its "beam"-decay constant λ^* (Z = 26) which can be extrapolated from neighbouring "stable" ions (solid curve in Fig. 7). For beta lifetimes less than $\sim 10^3$ s, however, this correction is marginal, because "beam" lifetimes of highly charged ions are in the order from 10^4 s (U^{92+}) to several 10^5 s (Ne^{10+}) for typical ESR-settings (pressure p $\approx 10^{-11}$ mbar, number of cooler electrons $\approx 10^6/cm^{-3}$).

The "Schottky lifetime spectroscopy" in the ESR of unstable, cooled highly charged ions is presently restricted to halflives $T_{1/2} \geq 30$ s (see 4.1.2). Much shorter β lifetimes can be addressed, however, by a rather simple and direct method: Since $\beta^{\pm}$ decay (but not bound-state beta decay nor EC) alters the ionic charge state and, hence, the ion trajectory, a particle detector moved to a well-defined position of the ring aperture may record

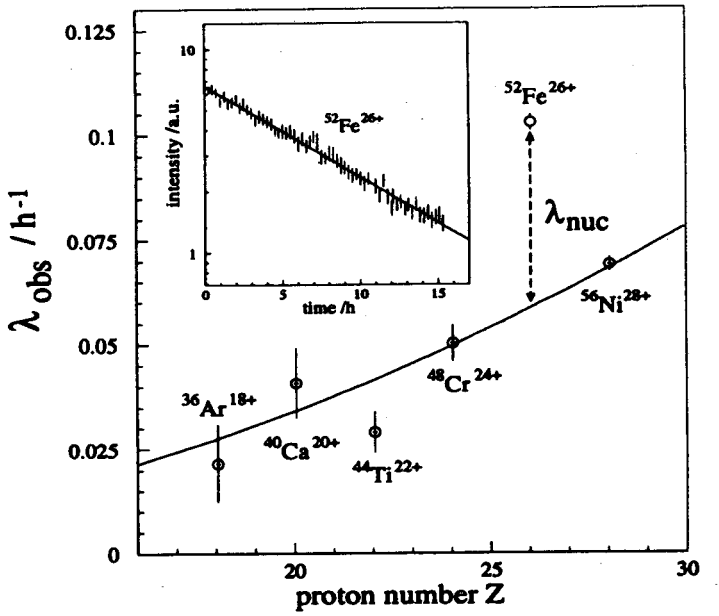

Fig. 7. Observed total decay constants λ_{obs} of simultaneously stored bare ions. The full line is a fit of an assumed $\lambda^* \propto Z^x$ dependence for the beam-loss probability $\lambda^*(Z)$. In this fit all data are included, except $^{52}Fe^{26+}$, which is the only isotope in the series where the nuclear decay constant λ_{nuc} is comparable to λ^*, ($\lambda_{obs} = \lambda^* + \lambda_{nuc}$). The insert shows the decay curve of $^{52}Fe^{26+}$, observed over more than 15 hours (from Ref. [4].

the daughter ions. Beta lifetimes down to the region of milliseconds are accessible by this simple technique, because cooling is not necessary. On the other hand, this method can only work if one single ion species (or at least one single short-lived species) is stored in the ring. An example is discussed in Ref. [34], where the β^+ lifetime of bare ^{19}Ne ($T_{1/2} = 17$ s) could be determined with an accuracy of 2 % (in a short parasitic experiment).

A long-term goal of lifetime measurements of highly charged unstable ions at the ESR is to reach an accuracy in the order of 1 part in thousand, by improving the detection technique and by reducing the inherent systematical errors (better calibration of Schottky peaks and of beam losses). If this level of accuracy would be accessible, challenging questions of nuclear physics and astrophysics could be addressed: For instance, precision lifetime measurements of pure Fermi ($0^+ \rightarrow 0^+$) transitions (*e.g.* $^{14}O \overset{\beta^+}{\rightarrow} {}^{14}N$), or EC decay probabilities of atoms with one, two ... electrons (*e.g.* $^7Be^{3+}$, $^7Be^{2+} \overset{EC}{\rightarrow} {}^7Li^{2+,1+}$).

5.2. Bound-state beta decay

The theory of β-decay usually assumes that the transformation of a neutron into a proton (or, in terms of the standard model, of a d-quark into a u-quark) is accompanied by the creation of an electron and an antineutrino which are both in continuum states and which share out with each other the Q-value of the decay. In this picture, however, those decays fail to appear in which an electron is created in a previoulsy unoccupied *bound* atomic state (bound-state β^- decay or, briefly, β_b-decay). Apparently, β_b-decay is the time-mirrored orbital electron capture (EC) and, therefore, closely connected with the latter by the principle of detailed balancing. This means in particular that EC and β_b-decay show indeed the identical nuclear transition matrix element $|M_{fi}|^2$ — provided of course that these transitions connect corresponding nuclear states — but differ with respect to phase-space factors and Q-values. In sharp contrast to continuum β^- decay (β_c-decay), EC as well as β_b-decay are two-body decays producing *monochromatic* neutrinos (EC) or, respectively, antineutrinos (β_b-decay) in the exit channel.

β_b-decay has been first predicted by Daudel, Jean, and Lecoin [38] in 1947 and, 14 years later, discussed comprehensively by Bahcall [39].

In neutral atoms, where the inner atomic orbits are "Pauli-blocked" and where only weakly bound states are available for the electron, β_b-decay is almost of no importance in comparison with continuum decay. Bahcall [39] has calculated, for instance, for the β^--decay $^3\mathrm{H} \rightarrow {}^3\mathrm{He}$ a relative fraction of $\sim 10^{-2}$ of β_b-decay, and for the β_b-decay of a neutron into a *neutral hydrogen atom* a fraction of a few ppm only with respect to its continuum β^--decay.

The situation is changing drastically, however, when going to highly ionized atoms with empty inner shell states (K,L ...):

- Most of total β^- decay probabilities will be enhanced considerably with respect to neutral atoms because of the enlarged Q-value for transitions to deeply bound states and because of the high probability density at the site of the nucleus of those states.
- β^- decay probabilities might change dramatically in cases where a β_b-transition to an *excited* state in the daughter nucleus with favourable selection rules will become possible, which is energetically *not* allowed in the corresponding neutral atom (*e.g.* $^{187}\mathrm{Re}^{75+}$, $^{205}\mathrm{Tl}^{81+}$ ...).
- Nuclei which are *stable*, if embedded in a *neutral* atom, might become *unstable* by β_b-decay if they are highly ionized (*e.g.* $^{163}\mathrm{Dy}^{66+}$, $^{205}\mathrm{Tl}^{81+}$, $^{160}\mathrm{Gd}^{64+}$ ...).

For these reasons β_b-decay has played, undoubtedly, a key role during nucleosynthesis in stellar plasmas at temperatures between a few keV and

some 100 keV, where the mean charge state of the atoms was very high.

5.2.1. First observation of bound-state beta decay

Bound-state beta decay was observed for the first time at the ESR, at the example of bare $^{163}Dy^{66+}$ [37]. (Note that *neutral* ^{163}Dy is absolutely stable).

For the experimental observation of β_b-decay up to 10^8 bare $^{163}Dy^{66+}$ ions of 294 MeV/u were accumulated, stored and cooled with electrons in the ESR. During the storage the β_b-decay daughters, stable hydrogen-like $^{163}_{67}Ho^{66+}$ ions, were continuously created. Having almost the same mass-over-charge ratio (A/q) as the primary ions, they were stored and cooled on the *same orbit*. The experimental procedure adapted by us to measure the number β_b-decay daughters, $^{163}_{67}Ho^{66+}$, was as follows: First, $^{163}_{66}Dy^{66+}$ ions were accumulated in the ring for a typical time of 30 min. Then an internal argon gas jet (thickness = $6 \cdot 10^{12}$ atoms/cm^2, diameter = 3 mm (FWHM)), which vertically crossed the beam, was turned on for about 500 s. By this action most of the $^{163}_{67}Ho^{66+}$ daughters produced during accumulation were removed from the closed orbit via electron capture or electron stripping. After the gas jet was turned off, the ions, the primary $^{163}_{66}Dy^{66+}$ as well as the decay products $^{163}_{67}Ho^{66+}$, were stored and cooled for a variable time t_s ranging from 10 to 85 min. The electron cooler was in operation during all stages of the experiment.

The detection and identification of these $^{163}_{67}Ho^{66+}$ daughters were based on the fact that *only they* could be further ionized, *i.e. only their* magnetic rigidity could be reduced. Therefore, in the last step the gas jet was turned on again in order to strip off the K electron in $^{163}_{67}Ho^{66+}$ and to detect the bare $^{163}_{67}Ho^{67+}$ either with a position-sensitive particle counter or via Schottky spectroscopy. From the number of $^{163}Ho^{66+}$ ions produced as a function of the storage time t_s and normalized onto the number of primary $^{163}Dy^{66+}$ ions, we got finally the bound-beta halflife (in the ion rest frame) of (48 ± 3) days.

5.2.2. Bound-state beta decay of bare $^{187}Re^{75+}$

The ^{163}Dy experiment in the ESR aimed, first of all, at the first experimental observation of bound-state beta decay. At the same time the overwhelming perspectives of well-running storage-cooler rings for doing this kind of "atomic astrophysics" could be demonstrated convincingly. Furthermore, the dramatic dependence of nuclear lifetime on the number of electrons was shown in a rather spectacular way.

There are, however, a few top-class problems in astrophysics which might be elucidated significantly by β_b-decay experiments. Those questions

concern, for instance, cross sections for solar neutrino absorption (β_b-decay of $^{205}Tl^{81+}$), or the effective life-time in a hot stellar plasma of atoms which serve as a galactic "chronometer" (^{187}Re). In both cases the β_b-decay of the highly ionized atoms ends in an *excited* state of the daughter nucleus. Therefore, the experimental determination of the β_b-decay probability is the *only way* to determine the unknown nuclear transition matrix element $|M_{fi}|^2$.

There is a long-lasting question of utmost importance in cosmology: How can one get a safe *experimental* — *i.e. not* model-dependent — lower limit T_u^{Min} for the age of the universe ? Today's "clocks" which could give bounds on T_u are

1. the abundance-ratio of long-lived radionuclides
2. globular clusters the age of which is estimated from luminosity/metallicity relations

The latter "clock" suffers from the same problem as suffers the Hubble constant H_0 itself, namely the never removed trouble on the *real* distance of very far objects [40].

Radionuclides in common use as "clocks" for T_u are ^{232}Th ($T_{1/2} = 14 \times 10^9$ yr $\equiv$ 14 Gyr), ^{238}U ($T_{1/2} = 4.5$ Gyr), and $^{187}Re/^{187}Os$ ($T_{1/2}$ (β^-) = 43 Gyr).

In order to derive a lower limit T_u^{Min} for the age of the universe, one needs the relative abundancies, decay constants and production probabilities in nucleosynthesis of these "clocks". For the case of the Th/U clock, the production probabilities depend on the (not well known) details of their generation in the "r"-process. As a consequence, the lower limit for T_u, derived from the $^{232}Th/^{238}U$-pair, fluctuates from 7.6 to 10.6 Gyr, depending on the model used for site and duration of the "r"-process.

In 1969, Clayton [41] pointed out that this serious drawback of the Th/U-clock could be circumvented by choosing a clock which is *not* loaded with the problem of the (unknown) primary production probabilities. He proposed as a better "clock" the pair $^{187}Re/^{187}Os$ (where ^{187}Os is the β^--daughter of ^{187}Re), because for this mother/daughter relation the primary production probability of ^{187}Re drops out. The only numbers needed to get a lower limit for T_u are the ratio of (cosmogenic) ^{187}Os to ^{187}Re on the one hand, and the decay constant of ^{187}Re, λ_{Re} on the other hand. By collecting today's most precise data one gets, in a conservative approach, a very precise lower limit for T_u of $T_u^{Min} \geq 11.5$ Gyr.

However, in 1983 Yokoi and Takahashi [42] showed that it is most probably wrong to use in this context the decay constant of *neutral* ^{187}Re. They pointed out that highly ionized ^{187}Re — for instance in a high-temperature stellar environment — might decay by many orders of magnitude faster due to bound-state beta decay to the first excited state of ^{187}Os ($E^* = 10$ keV).

They calculated for bare $^{187}Re^{75+}$, assuming from systematics a (log ft)-value of 7.5, a β_b halflife for this transition of $T_{1/2}^{\beta_b} = 14$ yr [43], *i.e.* more than 9 orders of magnitude shorter than the corresponding halflife of neutral ^{187}Re (43 Gyr).

Based on this value, Yokoi and Takahashi *calculated* an effective halflife T_{eff}(Re) of 35 Gyr (instead of 43 Gyr for neutral ^{187}Re), by modelling the galactic "history" of rhenium: How often and how long during the galactic evolution was rhenium in a "hot" environment ? (This "modelling", being in some respect arbitrary, has to reproduce, on the other hand, the correct abundances of all isotopes).

An effective halflife of 35 Gyr reduces the lower limit T_u^{Min} for the age of the universe from 11.5 Gyr to 9.0 Gyr. By far the largest uncertainty in this calculation comes from the assumed (log ft)-value of 7.5 for the nuclear matrix element which might be uncertain within a factor of $\pm$ 0.5 (corresponding to an uncertainty in the lifetime by a factor 3). It is evident that an *experimental* value for the β_b halflife of bare ^{187}Re has an essential impact for the reliability of the "corrected" Re/Os-clock. (If the β_b halflife for *bare* ^{187}Re is known, the halflives for all other charge states can be calculated safely.)

Very recently, an experiment has been conducted at the ESR aiming on the measurement of the β_b halflife of bare $^{187}Re^{75+}$. The experiment followed very closely the procedure described for the β_b-decay of bare ^{163}Dy (see 5.2.1). The question was, however, whether a halflife in the order of 10 years or even more could be detected or not (note that the β_b halflife of ^{163}Dy is 48 days, *i.e.* two orders of magnitude shorter !).

Figure 8 shows a Schottky spectrum after a storage time of 2 h of bare ^{187}Re and after the internal gas jet has been turned on for 300 s (in order to strip-off the bound electron of the β_b-daughter $^{187}Os^{75+}$). Together with the primary beam and with nuclear reaction products from the gas target, a peak of $^{187}Os^{76+}$ can be seen undoubtedly. In contrast to all nuclear reaction products, the intensity of $^{187}Os^{76+}$ grows in proportion to the storage time, signalling its origin from bound-state beta decay. From a very preliminary data evaluation we get a halflife for β_b decay of bare ^{187}Re of roughly 30 years, significantly larger than the value of 14 years adopted by Yokoi and Takahashi.

If this value of $\sim$ 30 years would be confirmed by the final data evaluation, the effective lifetime of ^{187}Re (in the framework of the galactic evolution model of Yokoi and Takahashi) would be only marginally differ from the lifetime of neutral ^{187}Re (43 Gyr). Hence, the lower limit for the age of the universe, as derived from the Re/Os-clock, would remain nearby to the "old" value of $T_u^{\text{Min}} \geq 11.5$ Gyr.

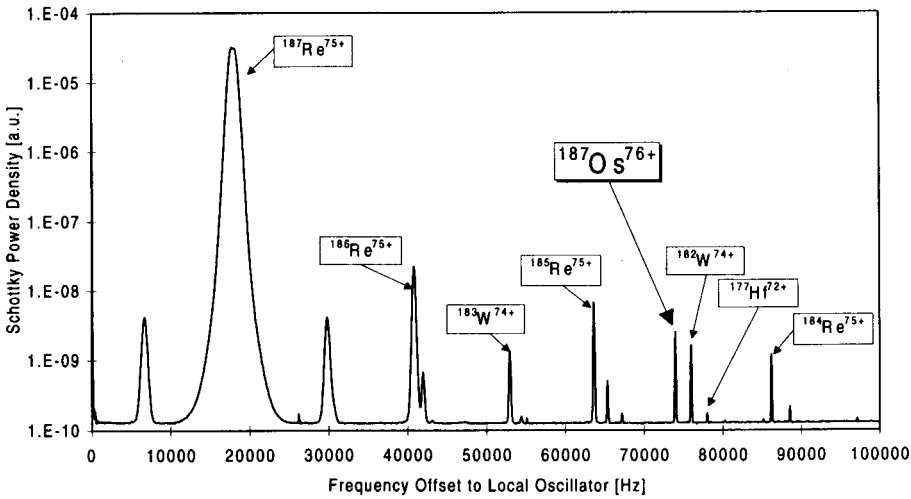

Fig. 8. Schottky spectrum after a storage time of 2 hours of bare $^{187}Re^{75+}$ in the ESR and after the internal gas jet (Ar) has been turned on for 300 s. Together with the primary $^{187}Re^{75+}$-beam and with nuclear reaction products from the gas jet, the β_b-daughter of ^{187}Re, ^{187}Os, can be seen clearly (in the gas jet the direct β_b-daughter $^{187}Os^{75+}$ was stripped to bare $^{187}Os^{76+}$).

REFERENCES

[1] V. Natarajan *et al.*, *Phys. Rev. Lett.* **71**, 1998 (1993).
[2] F. DiFilippo *et al.*, *Phys. Rev. Lett.* **73**, 1481 (1994).
[3] G. Bollen *et al.*, *Phys. Rev.* **C46**, R2140 (1992).
[4] H. Irnich *et al.*, *Phys. Rev. Lett.* (in print).
[5] P. Balling *et al.*, *Phys. Rev. Lett.* **69**, 1024 (1992).
[6] I. Klaft *et al.*, *Phys. Rev. Lett.* **73**, 2425 (1994).
[7] D.A. Church, *Phys. Rep.* **228**, 253 (1993).
[8] Proc. Nobel Symposium 91 on Trapped Charged Particles and Fundamental Physics, Lysekil 1994, Sweden, ed. I. Bergström, C. Carlberg, R. Schuch, *Phys. Scr. T* **59** (1995).
[9] Proc. "Cooler Rings and their Applications", ed. T. Katayama and A. Noda, World Scientific, Singapore 1991.
[10] R.S. Brown, G. Gabrielse, *Rev. Mod. Phys.* **58**, 233 (1986).
[11] H. Poth, *Phys. Rep.* **196**, 135 (1990).
[12] H. Danared *et al.*, *Phys. Lett.* **72**, 3775 (1994).
[13] G. Gabrielse *et al.*, *Phys. Rev. Lett.* **23**, 1360 (1989).
[14] H.F. Beyer *et al.*, GSI-90.20 Report, ISSN 0171-4546 (1990).
[15] D. Möhl *et al.*, *Phys. Rep.* **58**, 73 (1980).
[16] N. Beverini *et al.*, *Phys. Scr. T* **22**, 238 (1988).
[17] D. Wineland *et al.*, *Phys. Rev.* **A36**, 2220 (1987).

[18] S. Schröder *et al.*, *Phys. Rev. Lett.* **64**, 2901 (1990).
[19] D.J. Larson *et al.*, *Phys. Rev. Lett.* **52**, 70 (1986).
[20] D. Wineland *et al.*, *J. Appl. Phys.* **46**, 919 (0000).
[21] G. Savard *et al.*, *Phys. Lett.* **A158**, 247 (1991).
[22] C. Carlberg *et al.*, *IEEE Trans. Instr. Measurement* **44**, 553 (1995).
[23] G. Gabrielse *et al.*, *Phys. Rev. Lett.* **67**, 2504 (1986).
[24] R. Blümel *et al.*, *Nature* **334**, 309 (1988).
[25] F. DiFillippo *et al.*, *Phys. Scr. T* **59**, 144 (1995).
[26] R.S. Van Dyck *et al.*, *Phys. Scr. T* **59**, 134 (1995).
[27] G. Gabrielse *et al.*, *Phys. Rev. Lett.* **74**, 3544 (1995).
[28] C. Carlberg *et al.*, *Phys. Scr. T* **59**, 196 (1995).
[29] G. Audi et al, Nucl. Phys. **A449**, 491 (1986).
[30] D.J. Vieira *et al.*, *Phys. Rev. Lett.* **57**, 3253 (1986).
[31] A. Gillibert *et al.*, *Phys. Lett.* **B176**, 317 (1986).
[32] H. Stolzenberg *et al.*, *Phys. Rev. Lett.* **65**, 3104 (1990).
[33] G. Bollen, *Phys. Scr. T* **59**, 165 (1995).
[34] H. Geissel *et al.*, *Phys. Rev. Lett.* **68**, 3412 (1992).
[35] B. Franzke *et al.*, *Phys. Scr. T* **59**, 176 (1995).
[36] K.S. Balog *et al.*, *Nucl. Instr. Meth.* **B70**, 459 (1990).
[37] M. Jung *et al.*, *Phys. Rev. Lett.* **69**, 2164 (1992).
[38] R. Daudel *et al.*, *J. Phys. de Radium* **8**, 238 (1947).
[39] J.N. Bahcall, *Phys. Rev.* **124**, 495 (1961).
[40] K. Croswell, *New Scientist*, 13 Febr. 1993, p. 22.
[41] D.D. Clayton, Nature **224**, 56 (1969).
[42] K. Yokoi, K. Takahashi, *Astron. Astrophys.* **117**, 65 (1983).
[43] K. Takahashi, K. Yokoi, Nucl. Phys. **A404**, 578 (1983); K. Takahashi *et al.*, *Phys. Rev.* **C36**, 1522 (1987).